XLI CILAMCE
XLI Ibero-Latin American Congress on Computational Methods in Engineering
16-19 November, 2020 FOZ DO IGUAÇU PARANÁ - BRAZIL

Evaluation of Composite Hull for Subsea Separator

Rodrigo Duarte Ribeiro[1], Marysilvia Ferreira da Costa[1], Ilson Paranhos Pasqualino,[2], Olga M. O. de Araújo[3]

[1]*Dept. of Metallurgical and Materials Engineering, Federal University of Rio de Janeiro*
Av. Athos Silveira, 149 - CT - F Block - Room 214 - Cidade Universitária - Fundão Island, 21941-599, Rio de Janeiro, Brazil
rodrigoduarte@poli.ufrj.br, marysilvia@metalmat@ufrj.br
[2]*Dept. of Naval Architecture and Ocean Engineering, Federal University of Rio de Janeiro*
Av. Athos Silveira, 149 - CT - C Block - Room 203 - Cidade Universitária - Fundão Island - RJ, 21.945-970, Rio de Janeiro, Brazil
ilson@lts.coppe.ufrj.br
[3]*Dept of Nuclear Engineering, Federal University of Rio de Janeiro*
Av. Athos Silveira, 149 - CT - G Block - Room 206 - Cidade Universitária - Fundão Island - RJ, 21.945-970, Rio de Janeiro, Brazil
olgaufrjlin@gmail.com

Abstract. The subsea separator is one of the most important equipment to subsea processing, since it is responsible for separating the fluids extracted from the reservoir. The separation module may be composed by injection bombs and several other equipment, besides the separator tank, which makes it a huge structure. Since it is made of steel, the separator hull is extremely heavy and expensive, requiring very specific and expensive crane vessels for installation. Composite materials made of polymeric resins and fibers usually have very low density compared to steel, good mechanical properties, which make them a feasible alternative to weight reduction without losing structural safety. Therefore, it is important to evaluate its mechanical properties under the operational conditions to validate the proposed application. This work evaluated salt water absorption of composite plates under conditions of 3000 psi of external pressure and temperature of 4ºC. Tensile and shear tests were performed to assess the influence of water absorption on the resistance and elastic and shear moduli of the material. A numerical model was also developed to evaluate the behavior of the structure under different levels of external pressure and to compare a metallic with a composite hull. It was possible to conclude that the absorption did not cause significant changes on the elastic and shear moduli nor on the tensile strength of the material. In addition, the numerical results showed that, for the same external pressure, the composite hull has a thicker wall and a lower mass when compared with a metallic one.

Keywords: subsea separator, composite material, water absorption, aramid fiber, numerical simulation.

1 Introduction

Oil and gas exploration is one of the most expensive and most risky activities in the energy industry. When it comes to exploration in ultra-deep waters, the costs and risks are even greater. These environments require larger and more robust subsurface equipment with little or no intervention during their operational life. One of the most important equipment in a subsea processing site is the primary separator. It is composed of several pieces of equipment that are aggregated in a huge metallic structure responsible for separating the fluid from the reservoir into two or three streams of isolated fluids, facilitating and reducing the cost of production flow.
Steel is normally used to manufacture these equipment, which makes them extremely heavy, difficult to handle and makes deployment costs very expensive. However, alternative materials, such as composites, have been gaining ground in the industry due to their excellent mechanical properties, low density and other advantages over steel, as for instance, being free of corrosion and easily manufactured. Thus, the building of the separator hull with

these composite materials would lead to a reduction in installation and maintenance expenses and would increase safety in the equipment handling processes, since much lighter loads would be handled.
The paper is part of a comprehensive study to evaluate the feasibility of replace steel hulls by composite hulls as the main component of a subsea separator. To reach this aim several experimental tests were carried out with composite laminates to evaluate its structural strength under the operational conditions of high pressure, low temperature and salt water environment. In this case the main concern is the water absorption under the mentioned conditions and this effect on the material strength response. To simulate the operational condition a hyperbaric chamber was used during a test period of approximately six months. A finite element model was then developed to design the separator hull structure and to evaluate the effect of the water absorption on the mechanical response of the laminate.

2 Materials and Processing

Six composite plates were manufactured with dimensions 150 mm x 300 mm, as shown in Fig. 1. Half of the plates had fibers oriented at 0/90° and half had fibers oriented at ±45°. For each fiber orientation, samples were produced with 5, 10 and 15 layers of bidirectional plain-woven fabric of Kevlar 29 (aramid fiber).

Figure 1. Composite plates after lamination.

All plates were laminated with a polymeric matrix prepared by mixing two components: the epoxy resin Araldite® LY 1564 BR and the hardener Aradur® 2963, in a 2:1 volume ratio. The Kevlar® 29 fabric (model S745 Greige) was supplied by DuPont®, having a surface density of 439 g/m² and a thickness of 0.58 mm. The lamination method used was the wet lay up technique followed by vacuum bagging.

3 Experimental Procedure

The experimental part consisted of an absorption analysis, mechanical tensile and shear tests and a tomographic analysis before and after aging in the hyperbaric chamber.

3.1 Absorption Analysis

The manufactured composite plates were cut in half, had the edges sealed and were placed in a hyperbaric chamber containing artificial seawater. A temperature of 4 °C and pressure of 3000 psi (20.7 MPa) were used, considering a field application of 2000 m water depth.

The samples were kept pressurized during 189 days and were periodically removed from the chamber and weighted to assess absorption in terms of mass change. Ten weightings were carried out during this period. The apparatus used in the absorption test is shown in Fig. 2.

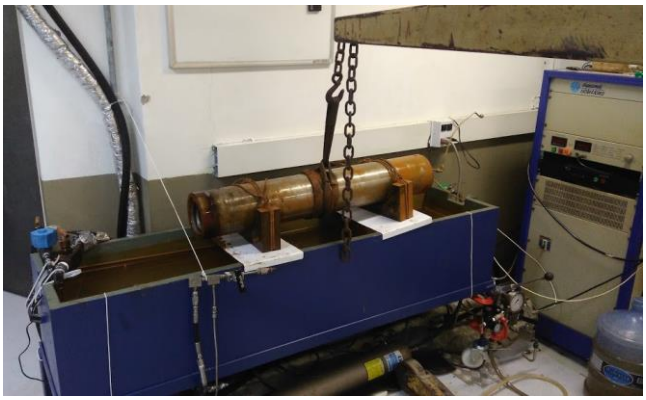

Figure 2. Apparatus used for the absorption analysis.

3.2 Material Characterization

To characterize the material, tensile and shear tests were performed before and after aging following the ASTM D3039 [1] and ASTM D3518 [2] standards, respectively. Elastic and strength properties were obtained and compared to evaluate the effect of water absorption on those properties. The mass and volume fractions of the materials were calculated using the ASTM D3171 [3] standard and the amount of pores were determined through tomographic analysis also before and after aging.

4 Numerical Analysis

A simplified numerical model was developed using the commercial finite element program Abaqus® to analyze the vessel behavior under different pressure conditions and to compare the response of a hull made of different materials. A three-dimensional (3D) shell was created with ½ circumference geometry, as can be seen in Fig. 3 (a). This simplification of geometry was chosen due to the model's symmetry planes and to reduce computational time.

The hull simulated has an internal diameter of 2.3 m and length of 7.0 m. The edges are perfectly circular while an ovalization of 0.5% was used in the center of the model to simulate construction imperfections and to avoid problems of non-convergence.

Two loads were applied to the model. The main one is the external pressure in the entire shell of the vessel. The other is a point force known as end cap effect, applied on one of the edges from the outside to the inside at a reference point in the center. A coupling function was used in order to transmit the effect of this force over the entire circumference of the edge. The external pressure applied, and for each one an overpressure of 30% was used as a safety factor.

Three materials were used in the numerical simulations: the composite of aramid fiber and epoxy resin experimentally characterized in this work, the synthetic polymeric foam Divinycell® HCP100 developed for submerged applications in sandwich structures and ASME A570 steel, which was considered to have perfectly plastic behavior. The properties of these materials can be seen in Tab.1.

The program was run for five depth configurations: 300 m, 500 m, 1000 m, 1500 m, and 2000 m. For each depth, a comparison of wall thickness and mass was performed for vessels with walls made of sandwich structure and made of ASME A570 steel.

The sandwich configuration can be seen in Fig 3 (b), where the faces are made of composite materials, with thickness e_f, and the core is made of a polymeric foam, with thickness e_n.

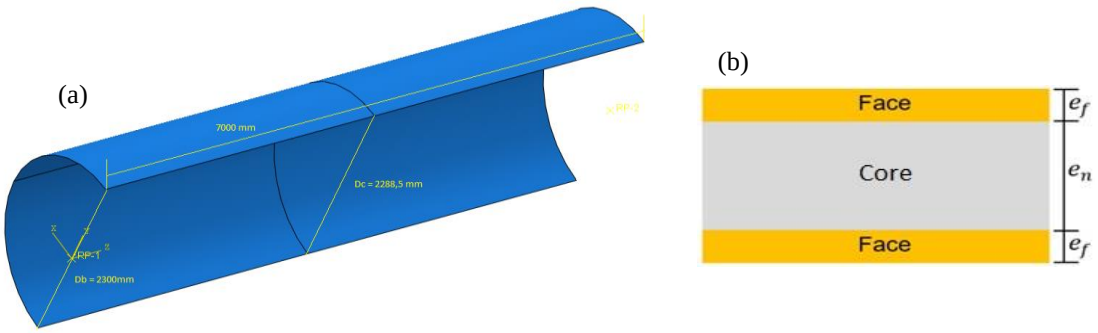

Figure 3. Numerical model geometry (a) and sandwich configuration (b).

Table 1. Property of materials used in numerical simulations.

Property (Mpa)	Composite	Core Foam	Steel
E_1	13485	650	191000
E_2	13485	650	-
ν_{12}*	0,23	0,3	0,3
G_{12}	1491	170	-
G_{13}	1000	170	-
G_{23}	1000	170	-
Yield Stress	-	-	586

*dimensionless

The model was meshed using elements type S4R, a four node linear quadrilateral shell element with reduced integration. A mesh size evaluation was performed comparing the Von Mises stress in a reference point and the total number of elements in the model. The result is shown in Tab.2.

Table 2. Mesh size assessment.

Element Size	Mises Stress (MPa)	Number of Elements
45	80,41	12.840
35	80,34	20.800
25	80,24	40.320
15	80,22	111.840

From Tab.2 it is possible to note that from element size 45 to 25, the Mises stress varies in the first decimal place. From 25 to 15, this variation happens in the second decimal place, showing a very small change in stress value. However, from size 25 to 15 there is a great increase in the number of elements, which also increases the computational time. So, the element size 25 was used in the model because of the good combination of accuracy and computational time.

5 Results

5.1 Absorption Analysis

Figure 4 shows the absorption curves for all specimens in terms of percentage of mass gain. The solid lines represent the composites with fibers at ±45° and the dashed lines represent the composites with fibers at 0/90°. The values in parentheses in the legend show the average thickness of each sample. The nomenclature of each sample is composed of two parts. The first one shows the angle of the fibers (0/90° or ±45°) and the second one

shows the number of plies in the sample (5, 10 or 15 plies).

The results show that the samples exhibited similar behavior of the absorption curve, with an initial linear absorption followed by a lower rate of increase that tends to equilibrium. It is observed, however, that none of the samples reached the saturation level during the 189 days of exposure.

Fickian absorption is characterized by an initial linear region followed by a plateau, where the material stop absorbing water (reaches saturation).

It is possible to notice that although the absorption curves are similar to Fickian absorption, it cannot be said that it was obeyed in any sample, since saturation was not reached.

According to Weitsman [4], the absorption process presented by the samples, with an initial linear region followed by a constant increase without reaching saturation, can be classified as Pseudo-Fickian.

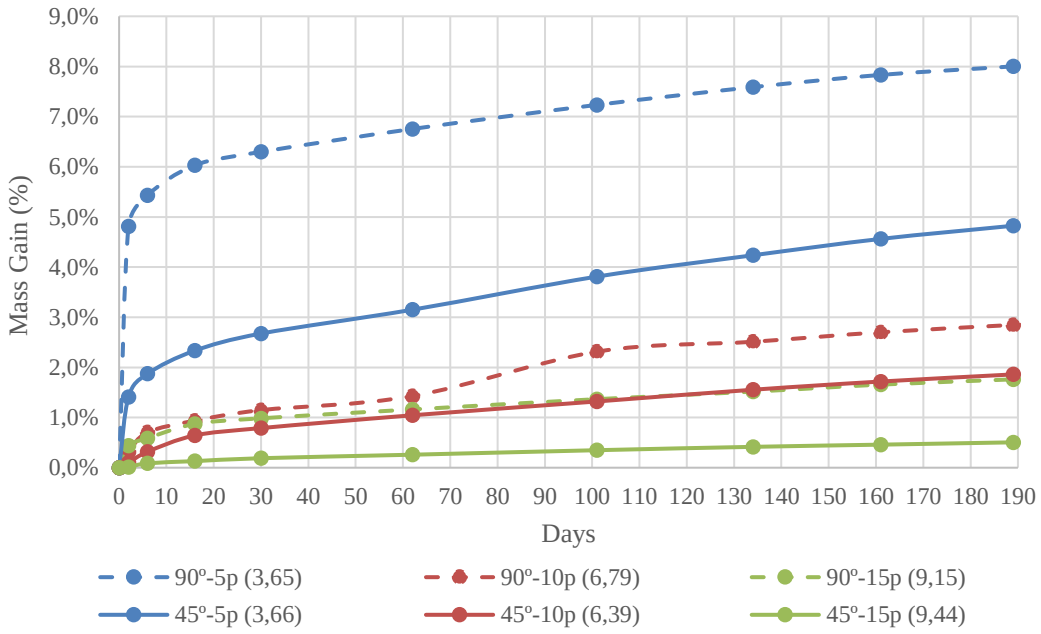

Figure 4. Absorption curves in terms of % of mass gain. Values in parentheses represent the average thickness of each sample.

5.2 Mechanical tests

The mechanical shear and tensile tests were performed in twelve specimens, six before aging and six after aging. Two specimens were tested for each number of plies. Table 1 shows the mean values calculated for the elastic and shear modulus. The percentage of variations is show in the last column, where the signs "+" and "-" means increase and decrease of the value, respectively. The nomenclature of the samples shows first the fiber orientation (0/90° or ±45º) and then the number of plies it contains (5, 10 or 15 plies).

Table 3. Mean values for elastic and shear modulus before and after aging and percentage of variation.

Samples	**Elastic Modulus (E) (GPa)**		
	Original	**Aged**	**Variation (%)**
0/90º- 5p	11,989	9,734	- 18,8 %
0/90º- 10p	11,105	11,448	+ 3,1 %
0/90º- 15p	14,368	13,485	- 6,2 %
	Shear Modulus (G) (GPa)		
±45º- 5p	1,149	1,104	- 3,9 %
±45º- 10p	1,177	1,146	- 2,6 %
±45º- 15p	1,330	1,491	+ 12,1 %

From Tab.3, it is possible to see that the water absorption generates a tendency to decrease the Elastic modulus, although this reduction is very small. The samples with 5 and 15 layers showed a small decrease in the modulus (18,8 and 6,2%, respectively), while the samples with 10 layers suffered a small increase (3,1%). However, as the variation found was very small, it cannot be said that such variation was caused by the absorption of water, since it may have occurred by other factors, such as the presence of internal defects or regions where there was a concentration of resin.

It can also be seen that the samples with 5 and 10 layers had practically no change in the shear modulus (3,9 and 2,6%, respectively). In turn, the sample with 15 layers showed a small increase (12,1%). It is noticed that the absorption of water has practically not altered the shear modulus of the material, being even less affected than the modulus of elasticity.

Table 4 shows the mean values for tensile strength calculated before and after aging and the percentage of variation.

Table 4. Mean values for composite tensile strength before and after aging.

Samples	**Strength (Mpa)**		
	Original	**Aged**	**Variation**
0/90º- 5p	339,625	341,278	+ 0,49 %
0/90º- 10p	302,946	327,163	+ 8,0 %
0/90º- 15p	336,435	338,946	+ 0,75 %

It can be seen that samples with 5 and 15 layers showed a slight increase in tensile strength in the order of 0,5 and 0,75%, respectively. The 10-layer sample increased by approximately 8%. This upward trend also cannot be fully credited to the water absorbed, since it is within the dispersion of the material.

5.3 Numerical Results

Figure 5 shows the hull intact (a) and the deformation after external pressure was applied (b).

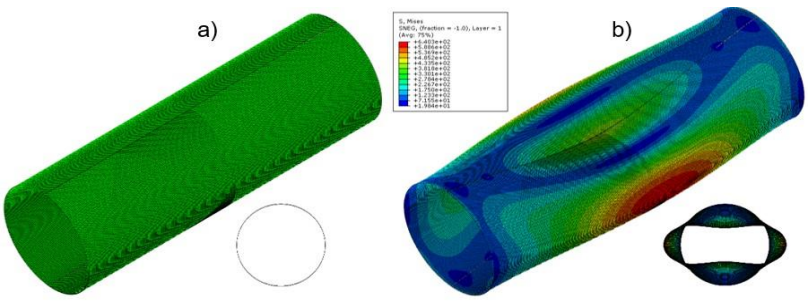

Figure 5. Hull before (a) and after (b) external pressure is applied.

A comparison between the metallic and sandwich hull can be seen in Fig. 6 (left). It shows the hull's wall thickness needed to withstand the external pressure of each depth. For the metallic one (orange line), the value in parentheses represents the thickness reduction in relation to the thickness of the sandwich hull (blue line).

Another comparison between the hulls can be seen in Fig. 6 (right), which shows the mass for each wall thickness configuration. It also shows the percentage reduction in mass of the sandwich hull compared to the metallic one.

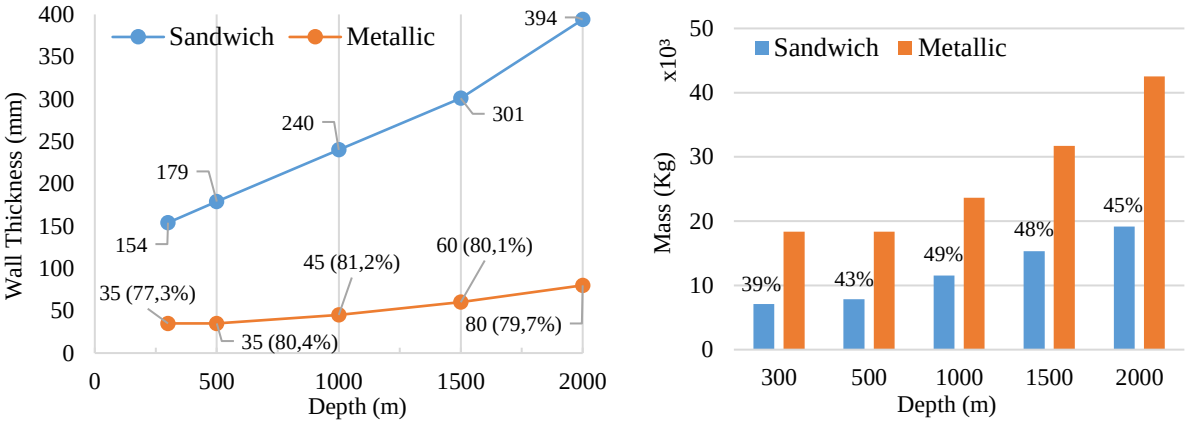

Figure 6. Comparison of wall thickness (left) and mass (right) between the sandwich hull (blue) and the metallic one (orange) for the five depths evaluated.

Analyzing Fig. 6 (left), it is possible to notice that the thickness of the sandwich vessel is much greater than the thickness of the metallic vessel. In contrast, Fig. 6 (right) shows that despite the greater wall thickness, the sandwich vessel has a significant reduction in mass compared to the metallic hull. For example, for the depth of 2000 m, the sandwich vessel has a mass reduction of 45% if compared with the metallic hull.

5.4 Porosity Analysis

Figure 7 shows the porosity images taken from the original sample 90°-5p showing the pore size distribution.

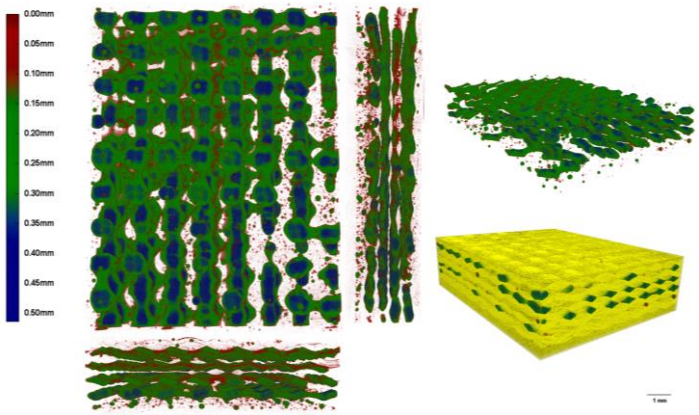

Figure 7. Pore size distribution in the original sample 0/90°-5p.

Table 5 shows a comparison of the porosity calculated by tomography for the samples before and after aging.

It can be seen that all samples showed a reduction in pore fraction, where samples with fibers oriented at ±45º showed a greater reduction than samples with fibers at 0/90°.

Table 5. Comparison of porosity for original and aged samples.

Samples	Porosity		
	Original	**Aged**	**Reduction**
0/90º- 5p	18,53%	16,81%	1,72%
0/90º- 10p	15,82%	-	-
0/90º- 15p	19,51%	18,59%	0,92%
±45º- 5p	18,21%	14,87%	3,34%
±45º- 10p	17,74%	-	-
±45º- 15p	17,72%	13,76%	3,96%

6 Conclusions

Hydrostatic tests showed that samples with fibers at 0/90° absorbed more water than those with fibers at ±45°, despite of being very close in thickness. This fact suggests that the fabric angulation may more or less influence absorption, however this hypothesis cannot be confirmed without carrying out additional experimental tests.

It was observed that the increase in the thickness of the samples generated a reduction in the diffusion rate and consequent decrease in the amount absorbed. It is believed that such behavior is due to the possible greater swelling suffered by the thinner samples, which generates more microcracks and facilitates the ingress of water. In addition, thinner samples are more susceptible to the appearance of cracks during the handling and cutting process.

The mechanical tests showed that water absorption had little influence on the elastic and shear modulus and on tensile and shear strengths.

The numerical analysis showed that the sandwich hull, despite having a greater wall thickness, has a mass considerably lower than a metallic hull due to the low density of the composite faces and the foam of the core.

In an ongoing study, if cost and manufacturing issues were taken into account, it is possible to say that sandwich structures made of composite laminate of aramid fiber and epoxy resin are strong candidates to the manufacturing of subsea separator hulls.

Acknowledgements. The authors would like to thank CAPES for the financial support and DuPont® for providing the aramid fiber.

Authorship statement. The authors hereby confirm that they are the sole liable persons responsible for the authorship of this work, and that all material that has been herein included as part of the present paper is either the property (and authorship) of the authors, or has the permission of the owners to be included here.

References

[1] ASTM D3039, 2014, “Standard Test Method for Tensile Properties of Polymer Matrix Composite Materials”, West Conshohocken, PA, EUA, ASTM International.
[2] ASTM D3518, 2013, “Standard Test Method for In-Plane Shear Response of Polymer Matrix Composite Materials by Tensile Test of a ±45° Laminate”, West Conshohocken, PA, EUA, ASTM International.
[3] ASTM D3171, 2015, “Standard Test Methods for Constituent Content of Composite Materials”, West Conshohocken, PA, EUA, ASTM International.
[4] Y. J. WEITSMAN. “Effects of Fluids on Polymeric Composites - A Review”. In: KELLY, A., ZWEBEN, C. (Eds.), **Comprehensive Composite Materials**. Vol II, Elsevier, pp. 369-401. 2000